8th International Colloquium on Bluff Body Aerodynamics and Applications
Northeastern University, Boston, Massachusetts, USA
June 7 - 11, 2016

Buffeting loads on high-rise and long-span structures

K. Hoffmann[a,*], R.G. Srouji[a], S.O. Hansen[b]

[a]*Svend Ole Hansen ApS, Copenhagen, Denmark,* kho@sohansen.dk*
[b]*SOH Wind Engineering LLC, Burlington, Vermont, USA*

SUMMARY:
Cross-sectional aerodynamic admittance functions for bridge decks may be determined in wind tunnels using section model testing. Full-scale prediction of the vertical buffeting load on bridges uses the cross-sectional aerodynamic admittance function measured in the wind tunnel together with conservative - sometimes too conservative - assumptions of the normalized co-spectrum of the lift forces. Many papers and text books emphasize that the lift force is better correlated than the vertical turbulence component, however the lack of accurate quantifications of "better correlation" increases the uncertainty of load predictions considerably. The buffeting load prediction procedure suggested in the paper reduces these uncertainties considerably by applying a more consistent description of the pressure correlations on bridge decks, and these more accurate predictions are especially relevant for long-span structures, such as modern cable-supported bridges. Wind tunnel experiments on a bridge section model are used to demonstrate the practical use of the derived stochastic model of buffeting loads.

Keywords: Buffeting loads, aerodynamic admittance, pressure correlation, large structures, size reduction function

1. INTRODUCTION

With the development of modern high-rise and long-span structures, engineers are facing an expanded array of design challenges. For such large structures, project costs, construction schedule, and the operational specifications are very much dependent on structural design criteria and thereby the ability of the engineers to accurately predict the considerable wind-induced loads of both static and dynamic character. An optimal design therefore requires load and response models accounting for the important physical principles associated with extreme structural dimensions. This is related to several parts of the wind-load chain; namely, the characteristics of the incoming wind, the aerodynamic response and the structural response (Hansen and Dyrbye, 1997).

Surface pressure fluctuations caused by turbulence in the atmospheric boundary layer are a key element in the generation of dynamic wind loads on structures. The governing turbulent flow mechanisms and the structural aerodynamic and mechanical characteristics jointly create the dynamic component of the resultant fluid-structure interaction. This is controlled by basic physical principles, yet it depends on a rather complex link between the incoming wind and the structural geometry. Understanding and predicting the nature of such buffeting wind loads is therefore crucial, since it ultimately provides designers and engineers the information necessary to assess structural safety and reliability, and to define operational requirements.

2. BACKGROUND

Structural loads on slender structures dominated by pressure differences, such as buffeting loads on tall buildings and bridge decks, are traditionally calculated using a quasi-steady approach, where

the resultant load is first estimated from time-averaged force coefficients based on the instantaneous relative wind direction in a suitable cross-sectional strip (Jakobsen, 1995). A spectral property of the buffeting load on the complete structure, such as the power spectral density, is then estimated using a frequency-dependent aerodynamic admittance function along the main structural dimension taking into account the reduced spatial correlation of surface pressures. It is most often tacitly assumed that surface pressures have a mean value proportional to the mean velocity pressure, have spectral properties similar to those of the incoming wind, are fully correlated along the cross-sectional strip, and have a correlation along the main structural dimension independent on the position on the strip. Various structure-dependent properties may be determined from wind tunnel measurements, but are often expressed by simplified representations, such as a flat plate approximation for streamlined bridge decks (Hansen and Dyrbye, 1997).

It is well-documented in the literature that the spatial pressure correlation description on a large building is different on the windward and leeward side relative to the mean wind direction (Hansen, 2012; Simiu and Scanlan, 1986). The spatial correlation between surface pressures on the windward side is largely dependent on the incoming turbulence characteristics, while the spatial correlation on the leeward side is largely dependent on the structural dimensions and geometry. It is simply a result of different characteristics of the flow generating positive and negative relative surface pressures. The cross-sectional strip typically used for buffeting response predictions will therefore often be a closed curve which in broad terms separates into parts, where the relative structural surface pressure is positive and negative, in the windward and leeward side of the instantaneous turbulent flow, respectively. The strip is therefore composed of several parts, each requiring a certain description of the spatial pressure correlation within each segment of the cross-section and along the main structural dimension. Actual differences between the physical flow characteristics responsible for the turbulence-induced forces at different parts of the structural surface is therefore not accounted for in the traditional approach, which involves the use of a single aerodynamic admittance function. It is, however, the opinion of the authors, that a response model must be consistent with basic physical principles governing the nature of the buffeting wind load. If not, it can only be prone to uncertainty and imprecision, especially for large structures, where the nature of surface pressure correlations may significantly influence predictions of both bending and torsional responses.

3. FORMULATION OF BUFFETING LOAD MODEL

To allow for a physically consistent description of the spectrally and spatially varying surface pressure distributions, the complete structural surface Ω is divided into non-intersecting sub-surfaces $\{\Omega_i\}_{i=1}^{N}$, each representing an area where the surface pressure characteristics are similar. For a rectangular building, this will typically correspond to the four vertical faces, and for a streamlined bridge deck, this will correspond to the top and bottom part.

The main principle of the proposed method relies on considering the buffeting wind load F_{t_i} on the sub-surface Ω_i in a chosen direction. The interaction between wind turbulence and the structural

mode of vibration is treated using a size reduction function approximated by the expression

$$K_{s_i}(n) = \frac{1}{1+\sqrt{(G_{y_i}\phi_{y_i})^2+(G_{z_i}\phi_{z_i})^2+\left(\frac{2}{\pi}G_{y_i}\phi_{y_i}G_{z_i}\phi_{z_i}\right)^2}}, \quad \phi_{y_i} = \frac{C_{y_i}b_i n}{U}, \quad \phi_{z_i} = \frac{C_{z_i}h_i n}{U}, \tag{1}$$

where n is the frequency, U is the mean wind velocity, C_{y_i} and C_{z_i} are decay constants for the normalized co-spectrum for the surface pressures, and the constants G_{y_i} and G_{z_i} are determined from the response of equivalent one-dimensional structures of length b_i and height h_i, respectively. This exponential format is usable for surface areas of both high-rise and long-span structures, with the correct asymptotes for frequencies approaching zero and infinity (Hansen and Dyrbye, 1997).

A summation of the fluctuating load contributions from all structural sub-surfaces then allows for an estimation of the power spectral density and the variance of the total fluctuating wind load in the chosen direction, expressed by

$$S_{F_t} = \sum_{i=1}^{N}\sum_{j=1}^{N}\sqrt{Coh_{F_{t_i}F_{t_j}}}\sqrt{S_{F_{t_i}}}\sqrt{S_{F_{t_j}}}, \quad \sigma_{F_t}^2 = \int_0^\infty S_{F_t}\,dn, \tag{2}$$

where $Coh_{F_{t_i}F_{t_j}}$ is the coherence between F_{t_i} and F_{t_j}. This calculation framework includes a load reduction caused by reduced correlation of surface pressures both within and between sub-surfaces.

Not only bending, but also buffeting-induced torsional loads may be of interest, especially for tall center-core buildings, including those having a symmetric cross section (Holmes, 2001). While the presented framework is perfectly usable for estimating such torsional buffeting loads, this paper presents example formulations for structures where vertical buffeting loads are of main interest.

4. WIND TUNNEL EXPERIMENTS

A series of boundary layer wind tunnel measurements have been performed to demonstrate typical applications of the derived buffeting model on a fixed structure. The results will be applicable on long-span structures for which the vertical buffeting loads are of main interest.

Wind tunnel tests have been conducted using a rigid pressure-tapped section model of a single box girder bridge deck in the wind tunnel facility located at Svend Ole Hansen ApS in Copenhagen, Denmark. The cross section is depicted in Fig. 1 along with the pressure tap locations.

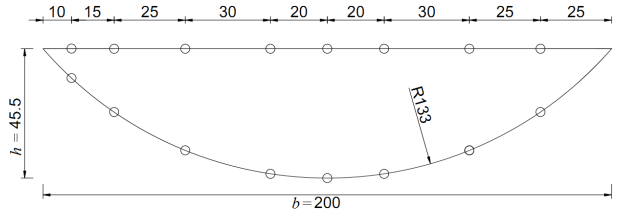

Figure 1. Location of pressure taps around section model and cross-sectional dimensions of the investigated single box girder. Dimensions are in model scale [mm].

The pressure measurements are conducted on a 1.70 m long section model. Seven longitudinal strips of pressure taps, denoted A to G, are installed parallel to the mean wind direction at the

1.10 m central portion of the section model, measuring fluctuating surface pressures; see Fig. 2. Each strip is fitted with 16 pressure taps distributed around the section model. The location of the strips is selected to provide sufficient resolution to determine the span-wise correlation of the surface pressures, which will be compared to measurements of the longitudinal and vertical components of the fluctuating wind flow. All tests were performed in turbulent flow with along-wind horizontal and vertical turbulence intensities of 15 % and 9 %, respectively.

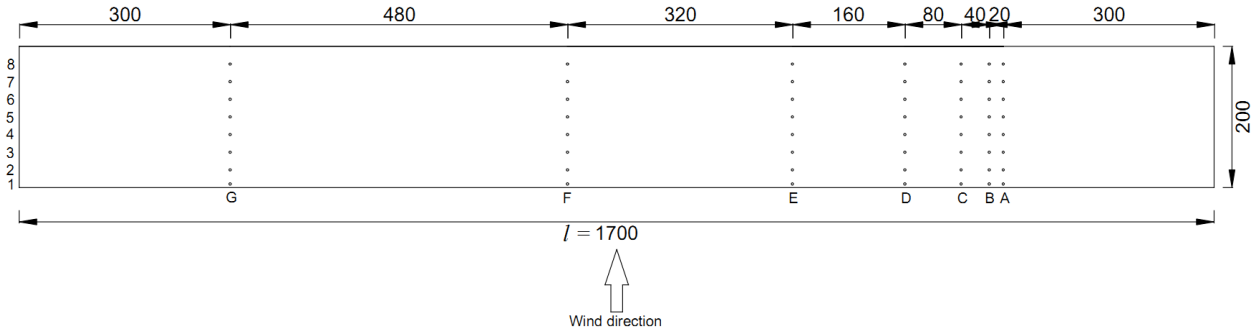

Figure 2. Location of the seven longitudinal and eight lateral strips. Dimensions are in model scale [mm].

5. RESULTS - VERTICAL BUFFETING LOADS

Temporal, spatial and spectral characteristics of the incoming wind and the generated structural buffeting surface pressures are related by the buffeting load physics. The present section addresses the wind tunnel investigation results obtained for the incoming wind turbulence and the pressure measurements on a sectional model of a single box girder bridge deck, in order to describe and model this physical interaction.

5.1. Wind characteristics

Establishing descriptions of the relevant characteristics of the turbulence components of the incoming undisturbed wind is the natural starting point for the analysis of buffeting loads. For vertical buffeting loads, this implies an analysis of the spectral and temporal characteristics of the longitudinal and vertical turbulence components for the chosen wind tunnel environment.

5.1.1. Spectral characteristics

A simple Fourier transform of the wind velocity signals allows for an estimation of the non-dimensional power spectral densities of the longitudinal and vertical turbulence components. These are presented in Fig. 3 and Fig. 4, respectively. On each figure, a von Kármán power spectral density function has been fitted to the results (Von Kármán, 1948), producing the following estimated integral length scales: $L_u^x = 0.90$ m and $L_w^x = 0.17$ m. Fitting an exponential decay to the autocorrelation function of the measured longitudinal and lateral wind turbulence yields similar estimates of the integral length scales, in accordance with Taylor's hypothesis.

Note that the ratio L_u^x/L_w^x in natural winds is normally found to be approximately two times larger than the ratio obtained from the values above. This discrepancy is caused by the spatial limitations of the wind tunnel environment reducing low-frequency vortices, corresponding to a decrease in L_u^x.

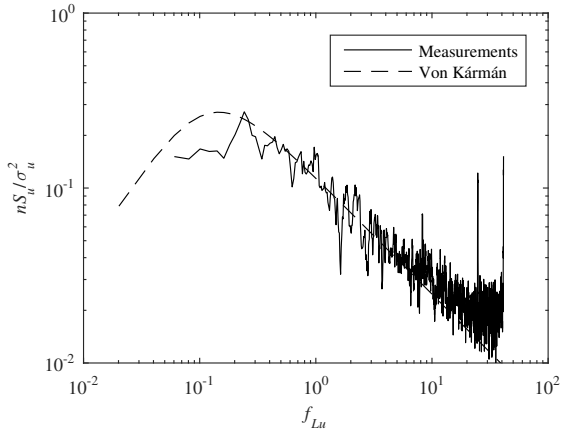

Figure 3. nS_u/σ_u^2 - Non-dimensional power spectral density of the longitudinal turbulence component u.

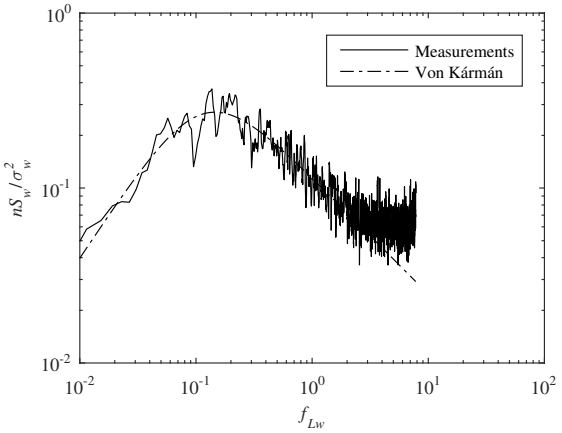

Figure 4. nS_w/σ_w^2 - Non-dimensional power spectral density of the vertical turbulence component w.

As a first approximation, the following length scales for lateral separations of the longitudinal and vertical turbulence are adopted (Strømmen, 2006): $L_u^y \approx \frac{1}{3} L_u^x = 0.30$ m and $L_w^y \approx \frac{3}{4} L_w^x = 0.13$ m, which facilities the description of wind turbulence correlations relevant for lift forces along the main dimension of long-span structures.

5.2. Buffeting load characteristics

Longitudinal and vertical turbulence components interact with the structure's geometry to generate spatially and temporally varying surface pressures, ultimately generating vertical buffeting loads. The buffeting load characteristics describe this interaction.

The power spectra associated with the fluctuating buffeting lift are related to the longitudinal and vertical turbulence spectra by (Hansen and Dyrbye, 1997)

$$S_{\text{Lift}}(n) = \left(\frac{1}{2}\rho U b l\right)^2 \left((2C_{\text{L}})^2 |\chi_u(n)|^2 S_u(n) + \left(\frac{dC_{\text{L}}}{d\alpha} + C_{\text{D}}\frac{h}{b}\right)^2 |\chi_w(n)|^2 S_w(n) \right), \tag{3}$$

where ρ is the air density, and for the present wind tunnel experiments: $U \approx 5.44$ $^{\text{m}}/_{\text{s}}$ the mean wind velocity, $C_{\text{L}} \approx -0.38$ the lift coefficient, $\frac{dC_{\text{L}}}{d\alpha} \approx 5.27$ the lift slope coefficient, $C_{\text{D}} \approx 0.60$ the drag coefficient, and $l = 1.70$ m, $b = 0.20$ m and $h \approx 0.05$ m are the cross-wind dimension, in-wind dimension and height of the section model, respectively. The admittance functions $|\chi_u(n)|^2$ and $|\chi_w(n)|^2$ model the lack of correlation between extreme pressures on the structural surface, generated by the longitudinal and vertical turbulence. The mathematical relation expressed by Eq. (3) is based on the assumption of zero correlation between the longitudinal and vertical turbulence components. The buffeting load predictions, especially at lower frequencies, may be improved if a more accurate turbulence correlation assumption is applied.

5.2.1. Longitudinal buffeting load correlations

The longitudinal correlation coefficients for buffeting loads on the top and bottom of the model are presented in Fig. 5. The results are based on measurements from a single longitudinal strip of pressure taps (Strip F; see Fig. 2), but a similar tendency is found for all seven longitudinal strips.

On the top part of the section model, the correlation is much homogeneous and seems to be somewhat similar to that of an exponentially format; see Fig. 5a. However, the correlation does not seem to approach unity, even for closely separated loads.

For the bottom part of the section model, the correlation coefficients have been divided into three sub-parts; see Fig. 5b. The correlation is shown relative to the buffeting load on the two points closest upstream (Points 1 and 2, positioned in Row 1 and 2; see Fig. 2), and between the remaining six points representing the more downstream part of the surface. The three different parts clearly illustrate their individual correlation properties. On the bottom of the model, the upstream buffeting loads are not much correlated to those located further downstream. The longitudinal correlation on the downstream parts is however significantly higher.

Load fluctuations in the longitudinal direction of the section model are not only generated from vertical and longitudinal wind turbulence, but also generated by the model itself in the form of vortices carried along the longitudinal direction by the mean flow. Harmonic model-generated pressure fluctuations, such as those originating the vortex shedding, are expected to be significant in the separated flow region on the downstream part of the bottom surface, which may explain the relatively large buffeting load correlations in this area. In areas where model-generated pressure fluctuations are generated more randomly, or are small in magnitude, such effects will reduce the correlation, which may be the case on the top.

The presented results indicate that the lateral correlation on the bridge deck cannot be encapsulated by a single exponential format. A consistent longitudinal buffeting correlation model may instead be based on a single description on the top, and two descriptions on the bottom, accounting for surfaces where either turbulence-induced and structure-generated load fluctuations are dominant.

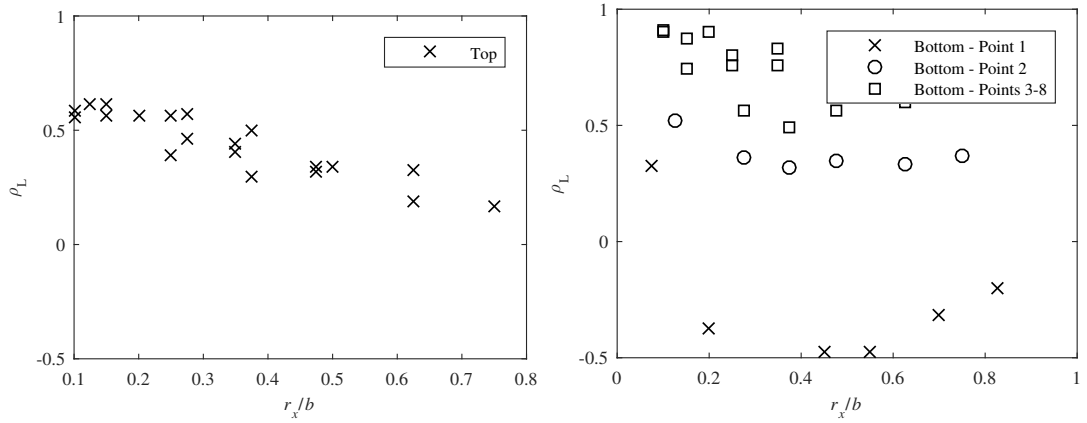

(a) Top **(b)** Bottom

Figure 5. Longitudinal buffeting load correlations on the top and bottom part of the section model for a single longitudinal strip. The longitudinal horisontal distance r_x is normalised by the section model width of $b = 0.20$ m.

5.2.2. Lateral buffeting load correlations

The lateral correlation coefficients for vertical buffeting loads along eight different lateral strips of the section model, and for the cross-sectional mean of the vertical loads, are presented in Fig. 6.

On each sub-figure, correlations for the top, bottom, and the sum of the top and bottom loads are presented. All loads are determined from surface pressures on a reference area having unit lateral extension. Considering the cross-sectional mean of the total top and bottom loads corresponds to the traditional approach, where a cross-sectional strip is treated as a point-like load for which the span-wise cross-sectional correlation is determined. Note that mean load is based on a weighting of each pressure measurement similar to the reference area it occupies.

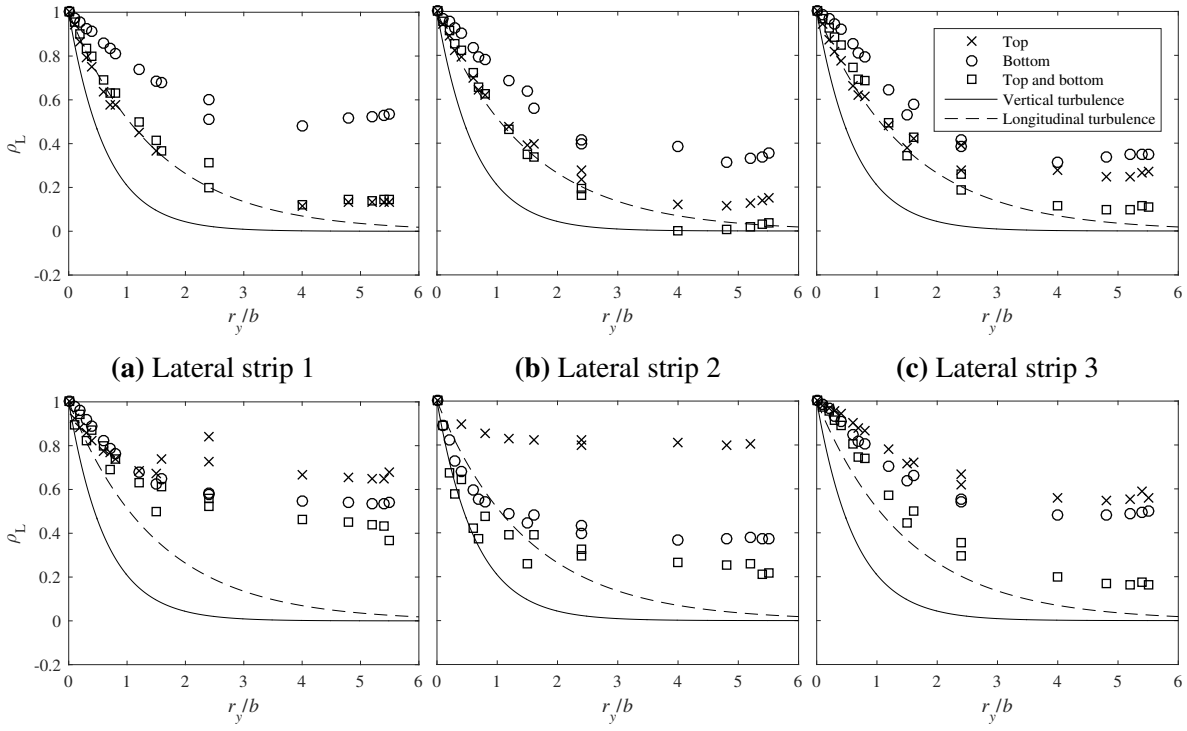

(a) Lateral strip 1 **(b)** Lateral strip 2 **(c)** Lateral strip 3

(d) Lateral strip 5 **(e)** Lateral strip 7 **(f)** Mean of lateral strips

Figure 6. Lateral correlation coefficients for point-like buffeting loads along five different lateral strips of the section model, and for the buffeting loads determined from line-like averaging on the top and bottom parts, and the complete cross-sectional mean. The lateral distance r_y is normalised by the section model width of $b = 0.20$ m.

Larger correlation are found on the bottom, especially distinct on the upstream part of the section model, where one would also expect longitudinal turbulence to be a more dominant source of buffeting loads. The fact that the combined top and bottom loads are systematically less correlated than the separate top and bottom loads indicates that different lateral correlation descriptions are necessary for the top and bottom part.

The lateral correlations of longitudinal and vertical turbulence are also plotted in Fig. 6. The buffeting loads are seen to be better correlated than the vertical turbulence, and in most situations also better correlated than the longitudinal turbulence. This property is well-documented in the bridge aerodynamics literature, and the traditional strip-wise buffeting load calculation takes this into account by the use of a lateral integral length scale 2-3 times larger than the associated length scale of the vertical turbulence (Hansen and Dyrbye, 1997). However, it may not be surprising that the buffeting load correlation differs from that of the vertical turbulence, since these loads are also

generated by the longitudinal turbulence, especially on the bottom part of the section model, and from vortices generated by the model itself. The non-dimensional power spectra of the longitudinal and vertical turbulence components may be converted into corresponding power spectra of point loads by utilizing the appropriate load coefficients; see also Eq. (3). Such power spectra of point loads due to longitudinal and vertical turbulence are presented in Fig. 7. Notice how the two spectra are separated spectrally and that the vertical turbulence are responsible for a large part of the power in the point load, especially for $\frac{nb}{U}$ larger than approx. 0.20.

By filtering the measured buffeting loads, it should therefore theoretically be possible to extract the loads generated by vertical turbulence. This has been done before calculating the lateral correlation coefficients depicted in Fig. 8. The loads are filtered to only contain normalized frequencies in the band $0.26 < \frac{nb}{U} < 1.48$, a part of the spectrum where the power of point loads due to vertical turbulence is much dominant to that of the longitudinal turbulence. The non-dimensional frequency range marked in Fig. 7 includes typical natural frequencies for vertical vibrations of bridges.

Tthe filtered cross-sectional load correlation is seen to follow the lateral correlation of the vertical turbulence. The lateral correlations for the top and bottom line-like loads seems to have an asymptotic correlation of approx. 0.30 for large separations. This may be caused by the positive correlation of loads in the cross-sectional direction, which is inherited by the longitudinal averaging performed to convert the line-like loads to point loads. This correlation is independent on the lateral separation, and may therefore manifest itself by the positive asymptotic behaviour of the correlation coefficient. However, when performing the averaging on the complete cross section a similar effect is apparently not present.

The presented analysis of the lateral buffeting load correlation indicates that when only considering buffeting loads generated by vertical turbulence, the span-wise correlation of cross-sectional loads may conveniently be described by the lateral correlation of the vertical turbulence.

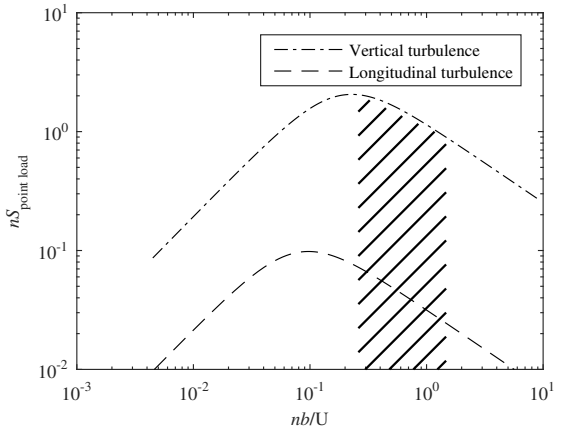

Figure 7. Power spectra of vertical point loads due to longitudinal and vertical turbulence. The shaded area illustrates the frequency band used to extract point loads primarily caused by vertical turbulence.

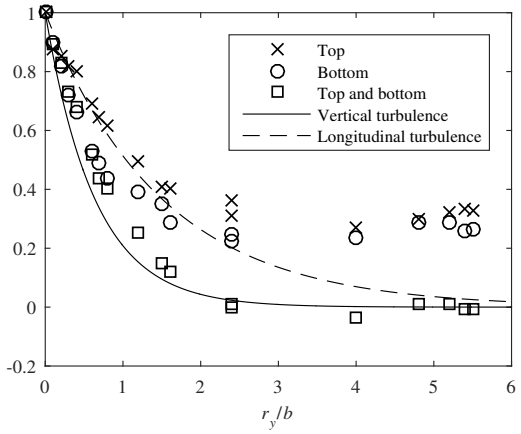

Figure 8. Lateral correlation coefficients for line-like averaged buffeting loads on the top and bottom, and the complete cross-sectional mean, for frequencies associated with vertical turbulence. The lateral distance r_y is normalised by the section model width of $b = 0.2$ m.

5.3. Aerodynamic admittance

The main focus of the present paper is to evaluate whether the span-wise aerodynamic admittance function χ^2_{L} for the lift forces may be based on characteristics of the vertical turbulence of the incoming, undisturbed wind.

Fig. 9 shows the aerodynamic admittance function measured in a single cross-section along with the Sears function. The Sears function is a theoretical reference of the cross-sectional aerodynamic admittance functions valid for a thin symmetrical airfoil (Sears, 1941). At low frequencies, the measured aerodynamic admittance function in a single cross-section is seen to differ from the theoretical Sears function. At the frequency of interest for cable-supported bridges, a good agreement is seen between the two admittance functions. In addition, Fig. 10 shows the aerodynamic admittance function for the full bridge, assuming the same lateral correlation of lift forces and of the vertical turbulence component. The very good agreement between the actual aerodynamic admittance function measured directly and the aerodynamic admittance function based on a measured cross-sectional aerodynamic admittance function and a span-wise aerodynamic admittance functions based on the vertical turbulence of the incoming, undisturbed wind is noteworthy. The agreement is particular good for nb/U values exceeding approx. 0.20, i.e. for buffeting loads primarily caused by vertical turbulence.

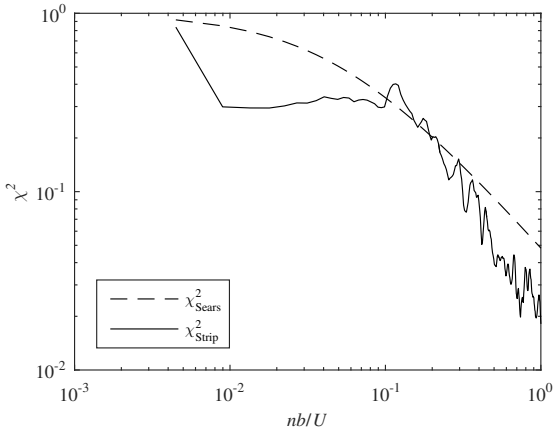

Figure 9. Cross-sectional aerodynamic admittance function. χ^2_{Sears} is the Sears function and χ^2_{Strip} is the admittance based on pressures measured in a single cross-section.

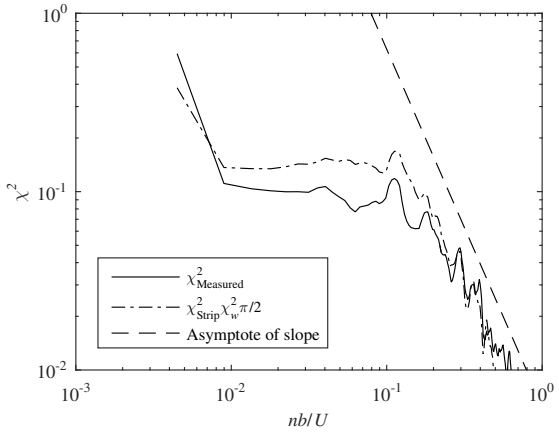

Figure 10. Aerodynamic admittance of entire bridge deck. $\chi^2_{\mathrm{Measured}}$ is the measured admittance, χ^2_{Strip} is based on pressures measured in a single cross-section and χ^2_w is the span-wise admittance for vertical turbulence of the incoming undisturbed wind.

For high frequencies, the exponential coherence function is normally used as an approximation of the normalized co-spectrum for turbulence components and pressures on structures. Using this assumption, the upper frequency limit of the aerodynamic admittance function may be determined as $\pi/2 \cdot \chi^2_{\mathrm{Strip}} \cdot \chi^2_{\mathrm{L}}$, where χ^2_{Strip} is the cross-sectional aerodynamic admittance function of the bridge deck and χ^2_{L} is the span-wise aerodynamic admittance function for the lift forces acting on the bridge deck. For the present type of bridge deck, the theoretical slope for high frequencies becomes $1/\phi_w \cdot 1/\phi_c$, where $\phi_w = C_w \cdot nl/U$ and $\phi_c = 2 \cdot \pi^2 \cdot nb/U$. C_w is the normalized co-spectrum decay constant for the vertical turbulence components with lateral separation and ϕ_c is based on the Sears

function. The asymptotic slope shown in Fig. 10 is seen to represent the measurements well.

The factor of $\pi/2$ is the ratio between the plate-like aerodynamic admittance function and the product of the two line-like aerodynamic admittance functions for high frequencies (Hansen and Dyrbye, 1997), and this factor is also included in the size reduction function given in Eq. (1).

6. CONCLUSION

The conducted analysis shows that the characteristics of pressure fluctuations generating buffeting loads on bridge decks varies along the structural surface. Areas where pressure fluctuations generated by either longitudinal turbulence, vertical turbulence or a flow/structure interaction are dominant, all require different stochastic buffeting load descriptions. The possible spectral separation of the corresponding loads, however, facilitates the analysis of loads from vertical turbulence, which is relevant for long-span bridges.

The accurate predictions of certain lateral load correlations, based on the characteristics of the incoming undisturbed vertical turbulence, is promising and it reduces the present prediction uncertainties considerably, especially for the frequency range where the vertical turbulence component is dominating. It is expected that similar results will be found for typical closed box-girder cross sections. On-going analyses will show to which extent these expectations will be fulfilled. The analyses will also cover possible prediction improvements obtained by dividing the cross section into subsections, e.g. by analyzing the top part and bottom part of the bridge cross section separately before the components are combined to give the final wind loads and responses on the entire bridge deck. The improved prediction accuracy will be beneficial for the design of cable-supported long-span bridges under consideration around the world.

ACKNOWLEDGEMENTS

The inspiring discussions with the Norwegian Public Roads Administration concerning consistent representations of aerodynamic admittance functions in bridge aerodynamics is highly appreciated.

REFERENCES

Hansen, S. O. 2012. “Wind Loading Design Codes”. Proceedings of *Fifty Years of Wind Engineering: Prestige Lectures from the Sixth European and African Conference on Wind Engineering*. Ed. by J. S. Owen, M. Sterling, D. M. Hargreaves, and C. J. Baker. Birmingham University Press.

Hansen, S. O. And Dyrbye, C. 1997. Wind Loads on Structures. John Wiley & Sons, New York, USA.

Holmes, J. D. 2001. Wind Loading of Structures. 1st ed. Taylor & Francis.

Jakobsen, J. B. 1995. Fluctuating Wind Load and Response of a Line-Like Engineering Structure with Emphasis on Motion-Induced Wind Forces. The Norwegian Institute of Technology, University of Trondheim, Norway.

Sears, W. R. 1941. Some aspects of non-stationary airfoil theory and its practical application. Journal of the Aeronautical Sciences 8, 104–108.

Simiu, E. And Scanlan, R. 1986. Wind Effects on Structures: An Introduction to Wind Engineering. Wiley-Interscience publication. Wiley.

Strømmen, E. 2006. Theory of Bridge Aerodynamics. Springer Berlin Heidelberg.

Von Kármán, T. 1948. Progress in the statistical theory of turbulence. Proceedings of the National Academy of Sciences of the United States of America 34, 530.